J Appl Electrochem (2008) 38:251–257
DOI 10.1007/s10800-007-9433-y

ORIGINAL PAPER

Electrochemical behavior of magnesium alloys AZ91D, AZCe2, and AZLa1 in chloride and sulfate solutions

**Guohua Wu · Yu Fan · Andrej Atrens ·
Chunquan Zhai · Wenjiang Ding**

Received: 25 September 2006 / Revised: 6 October 2007 / Accepted: 8 October 2007 / Published online: 16 November 2007

Abstract The influence of Cl^- and SO_4^{2-} on the electrochemical behavior of AZ91D, AZCe2, and AZLa1 was studied. For all alloys, there was a current plateau in the anodic polarization curves in Na_2SO_4 solutions. In 0.5% NaCl solution, there was a small current plateau, whereas there was none in the 3.5% and 5% NaCl solutions. This indicated that SO_4^{2-} is less aggressive than Cl^-. The range of the current plateau decreased with increasing SO_4^{2-} concentration. For all alloys, the high frequency capacitive loop in the Nyquist plots decreased with increasing concentration consistent with the decrease in corrosion resistance with increasing Cl^- and SO_4^{2-} concentration.

Keywords Magnesium · Corrosion · Chloride · Sulfate · Polarization · Electrochemical impedance spectroscopy

1 Introduction

Magnesium alloys have a high strength-to-weight ratio and Mg–Al alloys, such as AZ91D, show large promise for the automotive industry. Corrosion, however, limits the application of magnesium alloys [1–4]. Prior work has studied general corrosion and electrochemical behavior of AZ91 [5, 6], the influence of microstructure [7–9], corrosion product films [10–12], and the processing route [13]. Several studies [7, 9] have shown that the corrosion behavior is significantly influenced by microstructure, particularly the amount and distribution of the intermetallic phases. Our previous work [14, 15] showed that AZCe2 and AZLa1 had corrosion rates lower than AZ91D in salt spray or 5% NaCl solution. AZCe2 and AZLa1 are alloys based on AZ91D containing nominally 2% Ce or 1% La respectively.

There is not much information available concerning the influence of the environment. Only the work of Ambat et al. [16] studied the influence of chloride ion concentration and pH on the corrosion and electrochemical behavior of AZ91D. The present paper investigates the influence of Cl^- and SO_4^{2-} concentration on electrochemical behavior of the magnesium alloys AZ91D, AZCe2, and AZLa1.

2 Experiment

AZCe2 and AZLa1 were prepared from AZ91D, pure Ce, and pure La. AZ91D ingots were melted in an aluminum-

---

G. Wu (✉) · Y. Fan · C. Zhai · W. Ding
School of Materials Science and Engineering, Shanghai Jiaotong University, Shanghai 200030, P.R. China
e-mail: ghwu@sjtu.edu.cn; ghwu@hotmail.com

Y. Fan
e-mail: fyspy@sjtu.edu.cn

C. Zhai
e-mail: zhaicq@sjtu.edu.cn

W. Ding
e-mail: wjding@sjtu.edu.cn

A. Atrens
Materials, School of Engineering, The University of Queensland, Brisbane, QLD 4072, Australia
e-mail: andrejs.atrens@uq.edu.cn

A. Atrens
Swiss Federal Laboratories for Materials Science and Technology, EMPA, Dept 136, Überlandstrasse 129, 8600 Dubendorf, Switzerland

Table 1 Chemical composition of alloys (wt.%)

Alloy	Al	Zn	Mn	Ce	La	Fe	Ni	Cu	Mg
AZ91D	8.99	0.709	0.194	–	–	0.01	<0.002	<0.002	Bal.
AZCe2	9.05	0.684	0.215	1.953	–	0.0095	<0.002	<0.002	Bal.
AZLa1	9.12	0.672	0.179	–	1.064	0.0098	<0.002	<0.002	Bal.

oxide crucible at 730 °C under a flowing protective gas of 1 vol.% SF_6 in CO_2 and the appropriate amount of Ce or La was added to the molten AZ91D. The composition of AZ91D, AZCe2, and AZLa1 determined by ICP-AES, is presented in Table 1.

The specimens for electrochemical measurements, of dimensions 10 mm × 10 mm × 4 mm, were polished to 1,000 grit SiC paper and a wire was welded on the back surface for electrical contact. The specimens were embedded in epoxy resin so that about 1 cm^2 was exposed to the solution. The solutions, made with reagent grade chemicals and distilled water, were 0.5, 3.5, and 5 wt.% NaCl and 0.5, 3.5, and 5 wt.% Na_2SO_4. All solutions were saturated with $Mg(OH)_2$.

A Solatron 1287 + 1260 electrochemical measurement system was used for open circuit potential measurements, potentiodynamic scans, and electrochemical impedance spectroscopy (EIS). A three-electrode electrochemical cell was used, with a saturated calomel reference electrode and a platinum counter electrode. The potentiodynamic scans, at scan rate of 0.167 mV s^{-1}, were measured from $-$200 mV versus the corrosion potential to anodic potentials until the current density reached the preset value of 10 mA cm^{-2}. Electrochemical impedance spectra were measured at the corrosion potential, immediately after stabilization of the steady state potential, with an applied AC signal of 10 mV over the frequency range from 1 mHz to 1 kHz.

3 Results

3.1 Microstructure

The microstructure of as-cast AZ91D consists of primary α-Mg grains and large β ($Mg_{17}Al_{12}$) phase particles on the grain boundaries along with some fine β in a lamellar arrangement, Fig. 1a The microstructures of AZCe2 and AZLa1 were similar, except that AZCe2 and AZLa1 contained a greater amount of the β ($Mg_{17}Al_{12}$) phase in the fine lamellar arrangement. In addition, the microstructure of AZCe2, Fig. 1b, contained the rod-like phase Al_4Ce and the blocky phase $Al_{10}Ce_2Mn_7$ [14] and the microstructure of AZLa1, Fig. 1c, contained the rod-like phase $Al_{11}La_3$ and the blocky phase Al_8LaMn_4 [15].

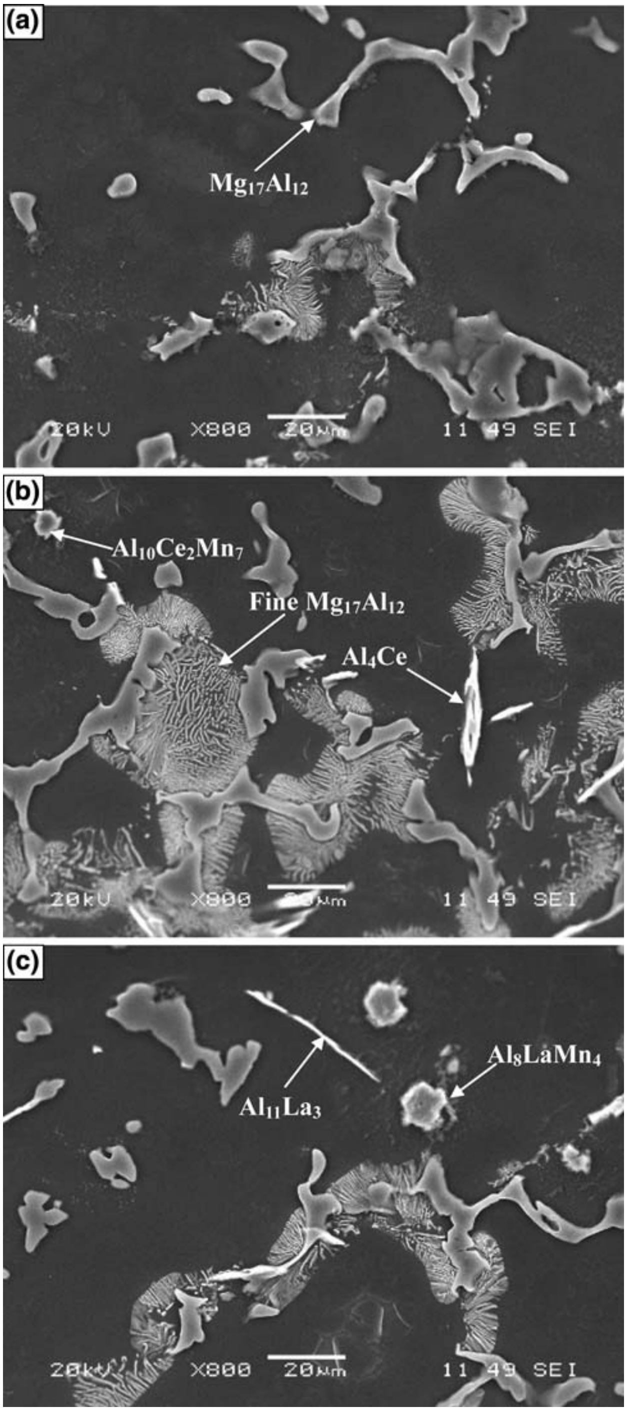

Fig. 1 Microstructure (SEM) of as-cast magnesium alloys: (**a**) AZ91D, (**b**) AZCe2, (**c**) AZLa1

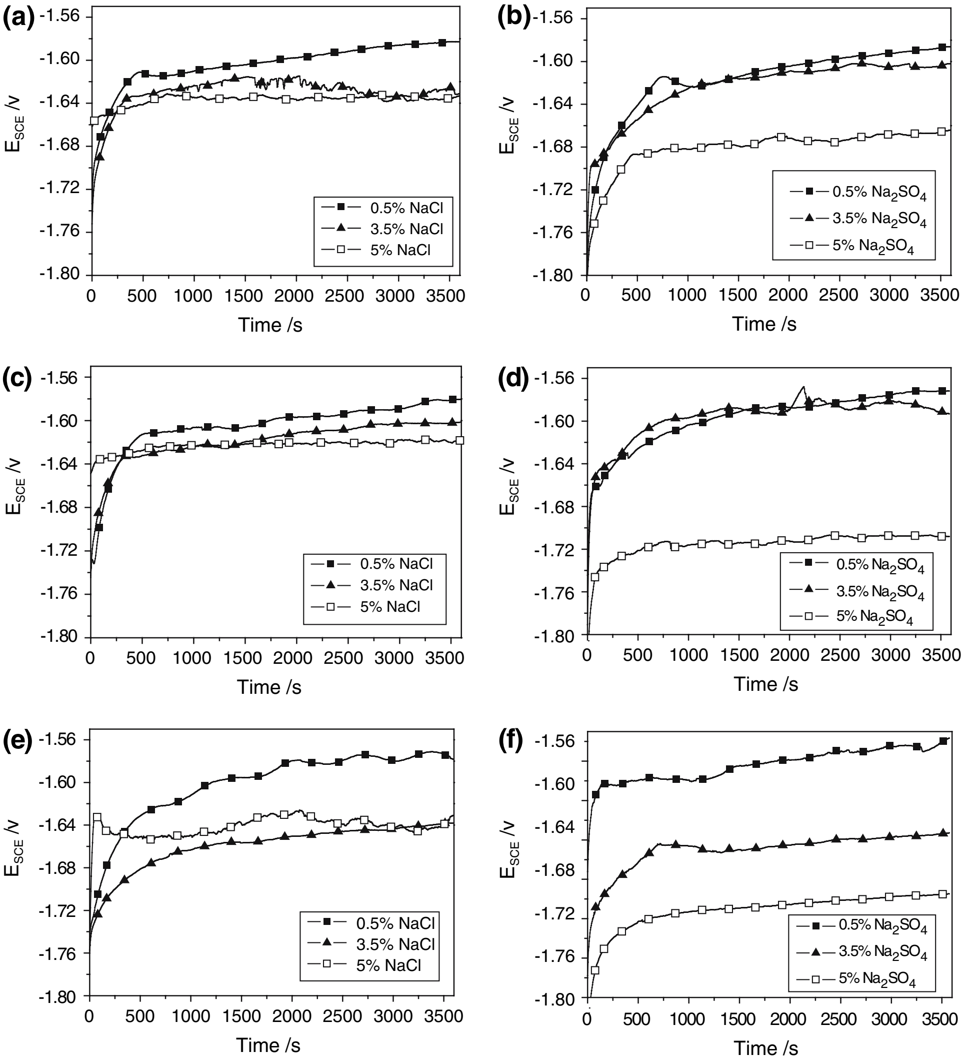

Fig. 2 Open circuit potential in NaCl or Na_2SO_4 solution saturated with $Mg(OH)_2$: (**a**) AZ91D in NaCl, (**b**) AZ91D in Na_2SO_4, (**c**) AZCe2 in NaCl, (**d**) AZCe2 in Na_2SO_4, (**e**) AZLa1 in NaCl, (**f**) AZLa1 in Na_2SO_4

3.2 Open circuit potential

The open circuit potential measurements for AZ91D, AZCe2, and AZLa1 are presented in Fig. 2 and the potential measured after 1 h immersion is reported in Table 2. The shape of all plots was similar. The potential rapidly increased during the first 15 min and then gradually tended toward a steady state value. For all alloys and for both solutions, the steady state potential was most positive in 0.5% solution. The steady state potential decreased with increasing concentration. For all alloys, the steady state potential in the NaCl solution was lower than that in the corresponding Na_2SO_4 solution except for the 5% solution. This may be attributed to the fact that Cl^- is more aggressive than SO_4^{2-}.

Table 2 OCP for AZ91D, AZCe2, and AZLa1 in NaCl and Na_2SO_4 solutions saturated with $Mg(OH)_2$

	OCP/V in NaCl			OCP/V in Na_2SO_4		
Alloy	0.5%	3.5%	5%	0.5%	3.5%	5%
AZ91D	−1.583	−1.631	−1.635	−1.586	−1.602	−1.664
AZCe2	−1.580	−1.601	−1.620	−1.572	−1.594	−1.708
AZLa1	−1.578	−1.636	−1.631	−1.535	−1.633	−1.695

3.3 Potentiodynamic polarization

The potentiodynamic polarization curves are presented in Fig. 3; they do not have symmetric anodic and cathodic branches. The cathodic curves followed Tafel behavior. The anodic curves were of two types: (i) a sharp increase after the corrosion potential and (ii) a current plateau after the corrosion potential. The current plateau indicated the existence of a partially protective surface film [17] although the current density values (10–200 μA cm^{-2}) are too high for a passive film. There was a current plateau for

Fig. 3 Polarization curves in NaCl or Na_2SO_4 solution saturated with $Mg(OH)_2$: (**a**) AZ91D in NaCl, (**b**) AZ91D in Na_2SO_4, (**c**) AZCe2 in NaCl, (**d**) AZCe2 in Na_2SO_4, (**e**) AZLa1 in NaCl, (**f**) AZLa1 in Na_2SO_4

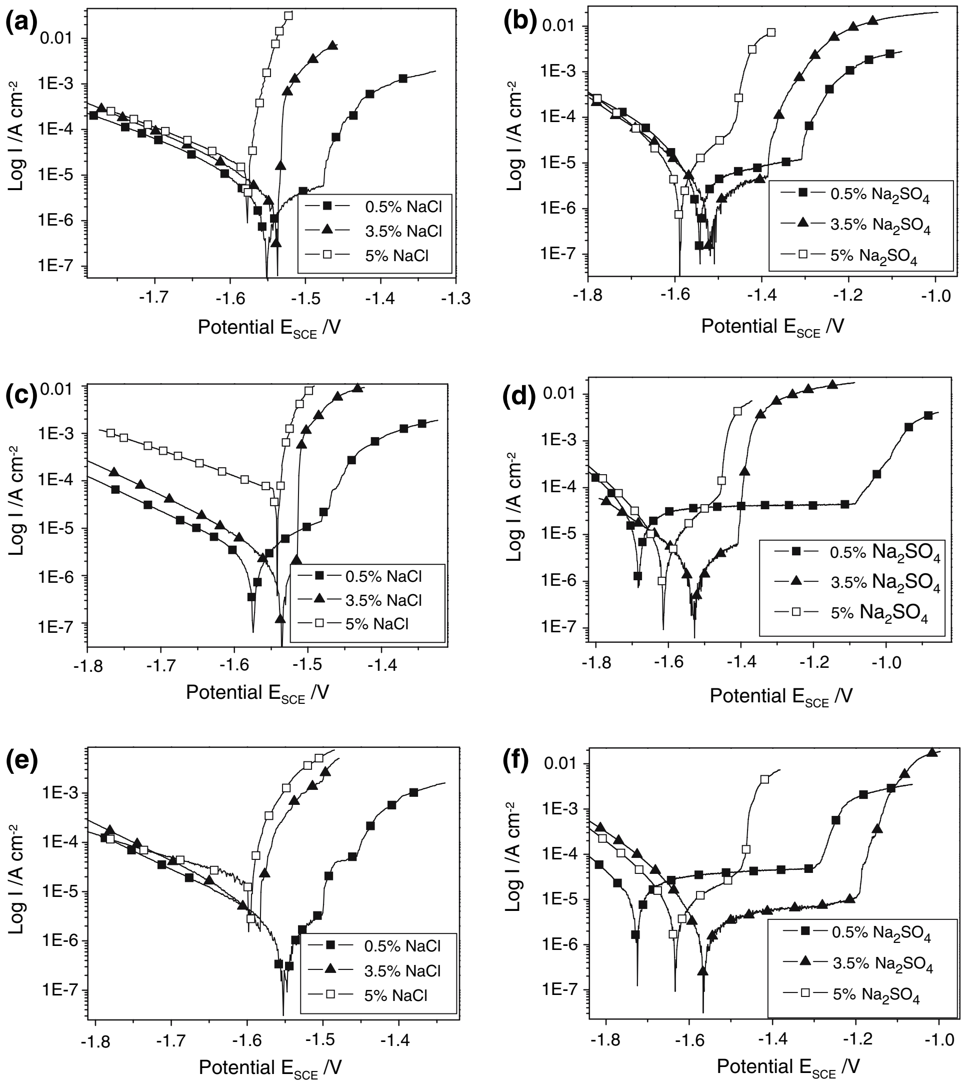

all the anodic curves in Na_2SO_4 solutions, although the plateau was small in the 5% Na_2SO_4 solution. In the NaCl solutions, there was no current plateau in 3.5% and 5% NaCl solutions; there was only a plateau in the 0.5% NaCl solution. This difference is attributed to the aggressive nature of NaCl solutions for magnesium alloys [18].

In the 0.5% Na_2SO_4 solution, the anodic polarization curve of AZ91D had a current plateau extending about 200 mV, whereas the current plateau for AZLa1 was over 300 mV and that for AZCe2 was more than 500 mV. This indicates that AZCe2 and AZLa1 had a corrosion resistance better than that of AZ91D, which is consistent with previous work [14, 15] in that the corrosion rates of AZCe2 and AZLa1 were both lower than that of AZ91D. The extent of the current plateau for AZ91D, AZCe2, and AZLa1 decreased with increasing SO_4^{2-} concentration.

The extent of the current plateau is limited by the breakdown potential, which corresponds to the breakdown of the surface protective film. In the 0.5% Na_2SO_4 solution, the breakdown potential for AZCe2 and AZLa1 was, respectively, −1.12 V and −1.28 V, which were both higher than that for AZ91D (−1.32 V). A more positive breakdown potential indicates a more protective layer. This suggested that the protective surface layer on AZCe2 and AZLa1 was more effective than that on AZ91D, which correlated with the higher corrosion resistance of AZCe2 and AZLa1.

3.4 Electrochemical impedance spectroscopy (EIS)

The EIS results are presented in Fig. 4. For all alloys, the Nyquist plots changed in a similar manner with increasing solution concentration. For all solutions except for 5% NaCl, the Nyquist plots for all alloys exhibited two capacitive loops: one high frequency capacitive loop and the other at low frequency. In the 5% NaCl solution, the Nyquist plots exhibit one high frequency capacitive loop

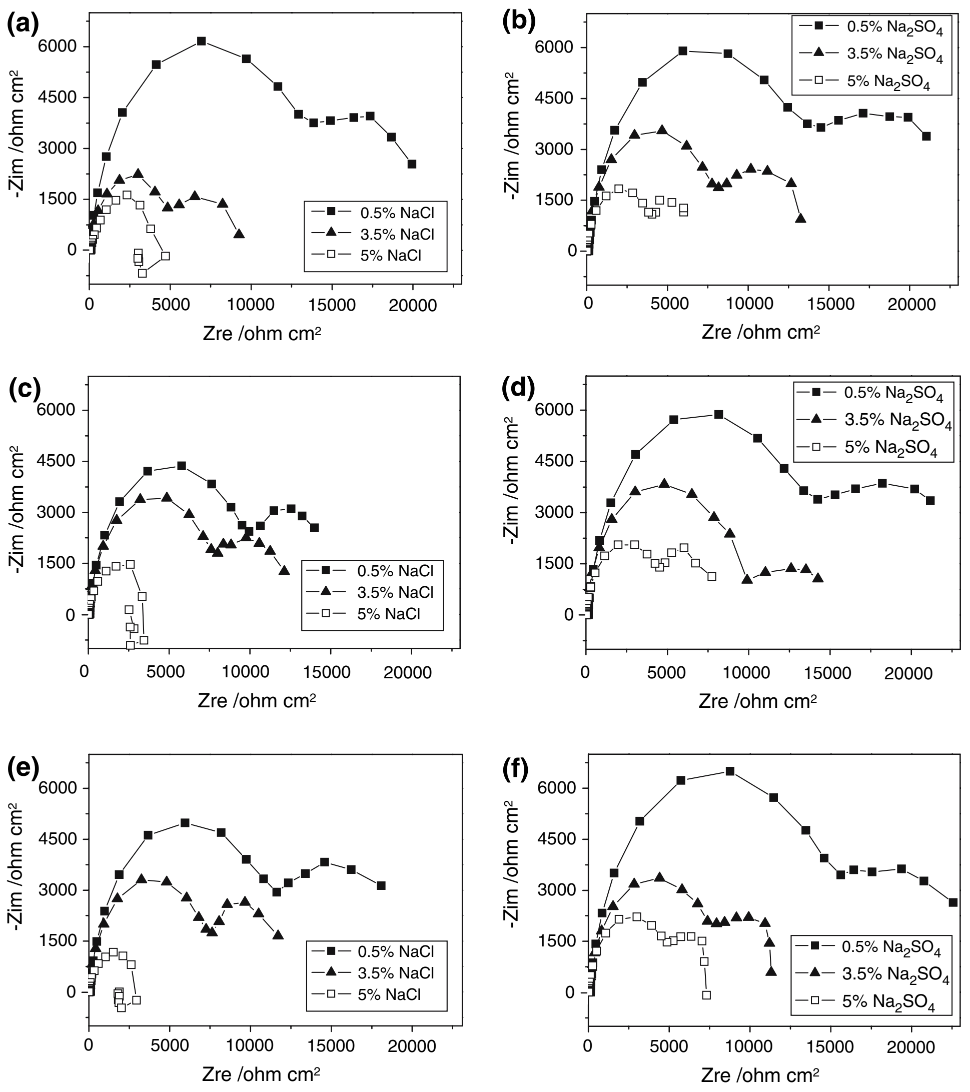

Fig. 4 Electrochemical impedance spectra in NaCl or Na_2SO_4 solutions saturated with $Mg(OH)_2$: (**a**) AZ91D in NaCl, (**b**) AZ91D in Na_2SO_4, (**c**) AZCe2 in NaCl, (**d**) AZCe2 in Na_2SO_4, (**e**) AZLa1 in NaCl, (**f**) AZLa1 in Na_2SO_4

followed by a small inductive loop at low frequency. According to Pebere and Riera [19], the high frequency capacitive loop results from both charge transfer and a film effect. The low frequency capacitive loop was attributed to a mass transport relaxation (probably Mg^+) in the surface layer. The inductive loop may result from absorbed species on the electrode surface [20].

The high frequency capacitive loop is related to the corrosion resistance. Makar et al. [21] showed that the corrosion rates calculated from the high frequency capacitive loop agreed well with weight loss measurements for a range of magnesium alloys. This means that the high frequency capacitive loop can be attributed to a charge transfer reaction. For all alloys, increasing Cl^- and SO_4^{2-} concentration led to a decrease in the size of the high frequency capacitive loop, which indicates that the corrosion resistance decreased. The decrease in corrosion resistance with increasing Cl^- and SO_4^{2-} concentration may be attributed to thinning of the partly protective $Mg(OH)_2$ surface layer.

The Nyquist plots in 5% NaCl solution were different from those in the other solutions. The impedance plots in 5% NaCl solution are consistent with the experiment results in 5% NaCl solution [14, 22]. A corroding metal can be modeled as a simple system consisting of a solution resistance, R_e, and a double-layer capacitance, C_d, in parallel with a charge transfer resistance, R_t; the equivalent circuit is shown in Fig. 5a. For the impedance diagrams with two capacitive loops, the appropriate equivalent circuit [23] contains two elements in series: (i) a charge transfer resistance, R_t (charge transfer), in parallel with the double layer capacitance, C_d, and (ii) a film capacitance, C_f, in parallel with a film resistance, R_f, Fig. 5b. These equivalent circuits were fitted using a method of parameter adjustment based on a simplex procedure. The correlation coefficient of fitting was at least 0.99. The values of R_t and

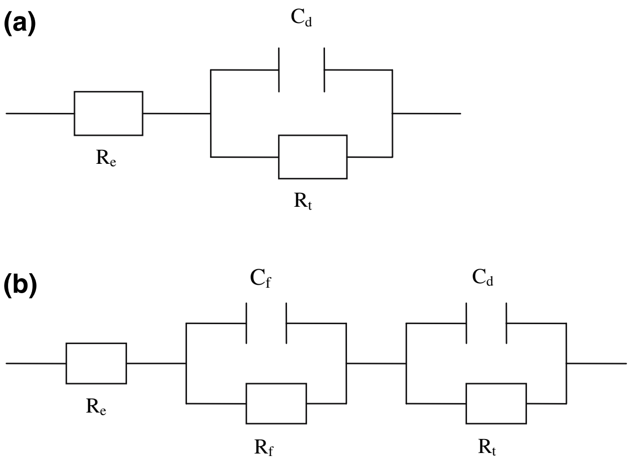

Fig. 5 Equivalent circuit for corrosion of the magnesium alloys in (**a**) 5% NaCl solution, (**b**) Na_2SO_4 solutions and 0.5%, 3.5% NaCl solution

Table 3 Charge transfer resistance, R_t for AZ91D, AZCe2, and AZLa1

	R_t/ohm cm^2 in NaCl			R_t/ohm cm^2 in Na_2SO_4		
Alloy	0.5%	3.5%	5%	0.5%	3.5%	5%
AZ91D	11590	4381	3251	11780	7436	3637
AZCe2	8832	7020	2855	12080	8907	4068
AZLa1	10540	6834	2159	13230	6478	4213

Table 4 Double layer capacitance, C_d for AZ91D, AZCe2, and AZLa1

	C_d/μF cm^{-2} in NaCl			C_d/μF cm^{-2} in Na_2SO_4		
Alloy	0.5%	3.5%	5%	0.5%	3.5%	5%
AZ91D	3.533	5.509	5.966	4.188	4.809	5.965
AZCe2	4.041	4.085	5.032	4.657	7.668	8.933
AZLa1	3.999	4.16	8.404	4.384	4.673	6.14

C_d are reported in Tables 3 and 4; R_t diminished rapidly with increasing concentration, whereas C_d slowly increased with increasing concentration. The decrease of R_t indicated a decrease in the corrosion resistance. The variation of C_d can be attributed to the high reactivity of the magnesium.

4 Discussion

The three magnesium alloys showed a current plateau in the anodic polarization curves in the Na_2SO_4 solutions. In the 0.5% NaCl solution there was a small current plateau on the anodic polarization, whereas there was no current plateau in 3.5% and 5% NaCl solutions. These results indicate that the SO_4^{2-} ion is less aggressive than the Cl^- ion. This agrees with the observation that sulfates attack magnesium to a lesser extent than chlorides [24, 25]. Song et al. [25] proposed that Cl^- greatly decreased the breakdown potential in 1 M NaOH solution. However, SO_4^{2-} had little influence on the passivation behavior of magnesium in 1 M NaOH, which indicates that SO_4^{2-} did not break the corrosion film. The authors suspected that chloride ion was involved in an intermediate magnesium dissolution step. The presence of chloride ion could make the surface film more active or increase the film-free area and might accelerate the electrochemical reaction rate from magnesium to magnesium-univalent ions.

For all alloys the OCP decreased with increasing Cl^- and SO_4^{2-} concentration. This result is different from that of the experiments of Song et al. [25], in which the corrosion potential of magnesium in 1 M NaOH slowly increased with increasing SO_4^{2-} concentration. This difference could be caused by the different solution. Song et al. used 1 M NaOH, which is strongly alkaline; whilst in this paper, the solution was saturated $Mg(OH)_2$. The strong alkaline solution causes magnesium to form an effective protective film, which reduces the corrosion of SO_4^{2-} .

For all alloys, the potential range of the current plateau was reduced with increasing SO_4^{2-} concentration. The high frequency capacitive loop decreased with increasing Cl^- and SO_4^{2-} concentration. These results indicate that the corrosion resistance decreases with increasing Cl^- and SO_4^{2-} concentration. This is consistent with the conclusion that the corrosion rate increases with increasing chloride ion concentration [16].

5 Conclusion

(1) The OCP for AZ91D, AZCe2, and AZLa1 decreased with increasing Cl^- and SO_4^{2-} concentration.

(2) For AZ91D, AZCe2, and AZLa1 there was a current plateau on the anodic polarization curves in Na_2SO_4 solution. However, in 0.5% NaCl solution, there was a small current plateau whereas there was none in the 3.5% and 5% NaCl solutions. This indicates that SO_4^{2-} is less aggressive than Cl^-.

(3) For AZ91D, AZCe2, and AZLa1, increasing Cl^- and SO_4^{2-} concentration led to a decrease in the high frequency capacitive loop. This indicates that the corrosion resistance decreases with increase in Cl^- and SO_4^{2-} concentration.

Acknowledgments This study was funded by the National Basic Research Program of China (973 Program) and National Key-technologies R & D Program of China.

References

1. Song GL, Atrens A (2003) Adv Eng Mater 5:837
2. Song GL, Atrens A (2007) Adv Eng Mater 9:177
3. Atrens A, Dietzel W (2007) Adv Eng Mater 9:292
4. Winzer N, Atrens A, Song GL et al (2005) Adv Eng Mater 7:659
5. Popov I, Starosvetsky D, Shechtman D (2000) J Mater Sci 35:1
6. Song GL, Atrens A, Wu X, Zhang B (1998) Corros Sci 39:1769
7. Song GL, Atrens A, Dargush M (1999) Corros Sci 41:249
8. Aung NN, Zhou W (2002) J Appl Electrochem 32:1397
9. Ambat R, Aung NN, Zhou W (2000) Corros Sci 42:1433
10. Fan Y, Wu G, Gao H et al (2006) J Electrochem Soc 153:B283
11. Nordlien JH, Nisancioglu K, Ono S et al (1996) J Electrochem Soc 143:2564
12. Nordlien JH, Ono S, Masuko N et al (1997) Corros Sci 39:1397
13. Mathieu S, Rapin C, Hazan J et al (2002) Corros Sci 44:2737
14. Fan Y, Wu G, Gao H et al (2006) J Mater Sci 41:5409
15. Fan Y, Wu G, C. Zhai (2006) Mater Sci Eng A 433:208
16. Ambat R, Aung NN, Zhou W (2000) J Appl Electrochem 30:865
17. Beldjoudi T, Fiaud C, Robbiola L (1993) Corrosion 49:738
18. Makar GL, Kruger J (1993) Int Mat Rev 38:138
19. Pébère N, Riera C, Dabosi F (1990) Electrochim Acta 35:555
20. Epelboin I, Gabrielli C, Keddam M et al (1975) Electrochim Acta 22:913
21. Makar GL, Kruger J, Joshi A (1988) In: Paris HG, Hunt WH (Eds) Advances in magnesium alloys and composites. TMS, p 105
22. Song GL, Bowles AL, Stjohn DH (2004) Mater Sci Eng A 366:74
23. Baril G, Pébère N (2001) Corros Sci 43:471
24. Song GL, Atrens A (1999) Adv Eng Mater1:11
25. Song GL, Atrens A, John DS et al (1997) Corros Sci 39:1981